Journal of Applied Polymer Science

Thermoresponsive Poly(γ-propyl-L-glutamate)-Graft-(oligo ethylene glycol)s: Synthesis, Characterization, and Properties

Yan Wu, Yong Deng, Qiulin Yuan, Ying Ling, Haoyu Tang

Key Laboratory of Polymeric Materials and Application Technology of Hunan Province, Key Laboratory of Advanced Functional Polymer Materials of Colleges and Universities of Hunan Province, College of Chemistry, Xiangtan University, Xiangtan, Hunan 411105, China

Correspondence to: H. Tang (E-mail: htang@xtu.edu.cn) and Y. Ling (E-mail: yingling0202@gmail.com)

ABSTRACT: A series of thermoresponsive poly(γ-propyl-L-glutamate)-graft-(oligo ethylene glycol)s (PPLG-g-OEGs) with different main-chain and side-chain lengths have been synthesized via copper-mediated alkyne-azide 1,3-dipolar cycloaddition between poly(γ-azidopropyl-L-glutamate)s (PAPLG) and propargyl terminated oligo ethylene glycols (Pr-OEGs). Fourier transform infrared spectrometer analysis revealed that $PAPLG_{10}$ adopted 39.4% β-sheet, 47.4% α-helix, and 13.2% random coil while PAPLG with longer main-chain length (DP = 37 and 88) and PPLG-g-OEGs adopted exclusive α-helix in the solid state. Circular dichroism analysis revealed that PPLG-g-OEGs adopted α-helical conformations with helicities in the range of 50∼100%. The thermoresponsive behaviors of PPLG-g-OEGs in water have been studied by dynamic light scattering. The polymer concentration, main-/side-chain length, and helicity collectively affected their cloud point temperatures. © 2014 Wiley Periodicals, Inc. J. Appl. Polym. Sci. **2014**, *131*, 41022.

KEYWORDS: properties and characterization; stimuli-sensitive polymers; structureproperty relations

Received 21 February 2014; accepted 13 May 2014

DOI: 10.1002/app.41022

INTRODUCTION

Thermoresponsive polymers are a class of polymers which undergo a solution phase transition on temperature variations.[1] They have been extensively studied for their potential applications as biomedical materials,[2] including thermoresponsive nanoparticles[3,4] and hydrogels,[5,6] and also in enhanced oil recovery.[7,8] Most known examples of thermoresponsive polymers with solution phase transition temperatures (i.e., cloud point temperatures) are poly(*N*-isopropylacrylamide) (PNIPAM), poly(*N*,*N*-diethylacrylamide), polyethers and poly(2-oxazoline)s.[1,9] The solution phase transition originates from a balance between attractive segment–water interactions and segment–segment interactions. It decreases as increasing segment–segment interactions or decreasing attractive segment–water interactions. However, polyacrylate or polyacrylamide based thermoresponsive polymers are nonbiodegradable, which restricts them in biomedical applications.

Synthetic polypeptides are mimics of natural peptides with biocompatible and biodegradable properties.[10,11] They have gained increasing interest for their significantly potential application as biomedical materials. They can fold into stable secondary structures (e.g., α-helix and β-sheet) in both solution and solid state. Additionally, they can be prepared by controlled ring-opening polymerization of *N*-carboxylanhydride (NCA) monomers.[12,13] Therefore, it will be interesting to develop polypeptides with thermoresponsive properties.[14,15] For examples, Li and coworkers reported thermoresponsive peglated poly-L-glutamate (i.e., poly-L-EGxGlu)[16] and peglated poly-L-cysteine (i.e., poly-EGxMA-C and poly-EGxA-C)[17] from ring-opening polymerizations of NCA monomers. Chen et al. reported a versatile synthesis of thermoresponsive polypeptides (PPLG-g-MEOs) by click reactions between poly(γ-propargyl-L-glutamate)s and azido functionalized oligo ethylene glycols.[18] These materials showed potential applications as smart carriers.[19] Yet, more effort is demanded to explore the relationship between molecular structures of polypeptides and their solution phase transition properties.

In this work, we report the preparation and properties of thermo-responsive poly(γ-propyl-L-glutamate)-graft-(oligo ethylene glycol)s (PPLG-g-OEGs) by click reactions between poly(γ-azidopropyl-L-glutamate)s (PAPLG) and propargyl terminated oligo ethylene glycols (Pr-OEGs). The successful preparation of the resulting samples has been characterized by proton nuclear magnetic resonance spectroscopy (^{1}H NMR), gel permeation chromatography (GPC), and Fourier transform infrared spectrometer (FTIR). The relationship between molecular structures and solution properties has been characterized by circular dichroism (CD) and dynamic light scattering (DLS).

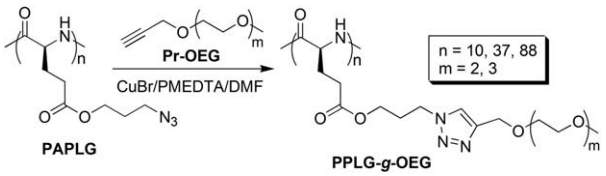

Scheme 1. The synthetic route of PPLG-g-OEGs.

EXPERIMENTAL

Materials

Poly(γ-3-azidopropyl-L-glutamate) (PAPLG)[20,21] and propargyl functionalized oligo ethylene glycols (Pr-OEGs)[22] were synthesized according to a reported procedure. CuBr (99%) and pentamethyldiethylenetriamine (PMDETA, 99%) were purchased from Energy Chemical. *N*,*N*-dimethyl formamide (DMF, >99.9%) and other chemicals were purchased from Aladdin and used as received.

Instrumentation

Proton nuclear magnetic resonance spectroscopy (^{1}H NMR) was recorded on a BRUKER ARX400 MHz spectrometer. Chemical shifts (δ) were reported in the units of ppm and referenced to the protio impurities in deuterated solvents. GPC measurements were performed on a PL-GPC120 setup equipped with a column set consisting of two PL gel 5 μm MIXED-D columns (7.5 × 300 mm, effective molecular weight range of 0.2∼400.0 kg mol^{-1}). DMF containing 0.01*M* LiBr was used as the eluent at 80°C at a flow rate of 1.0 mL min^{-1}. Narrowly distributed polystyrene standards in the molecular weight range of 0.5∼7.5 × 10^7 g mol^{-1} (PSS, Mainz, Germany) were utilized for calibration. FTIR was recorded on a Thermo Scientific Nicolet 6700 FTIR. CD measurements were performed on a JASCO J-700 CD spectrometer. The polymer samples were prepared at concentrations of 0.1 mg mL^{-1} in general unless otherwise specified. The solution was placed in a quartz cell with a path length of 0.2 cm. The mean residue molar ellipticity of each polymer was calculated based on the measured apparent ellipticity by following the literature reported formulas: Ellipticity ($[\theta]$ in deg·cm^2 dmol^{-1}) = (millidegrees × mean residue weight)/(pathlength in millimeters × concentration of polypeptide in mg mL^{-1}).[23] The helicity of the polypeptides were calculated by the following equation: helicity = $(-[\theta]_{222} + 3000)/39{,}000$.[24] DLS measurements were conducted on a BI-200 SM scattering system (Brookhaven instruments corporation) equipped with a digital time correlator (BI-9000), a laser (532 nm) at a scattering angle of 90°, and a controller (BI-TCD) for precisely adjusting the solution temperature. The solutions were heated in steps and stabilized for 10 min before light scattering intensity were recorded.

Synthesis of Poly(γ-propyl-L-glutamate)-Graft-(oligo-ethylene-glycol) (PPLG-g-OEG)

A representative experimental procedure is given as follows. PAPLG (30 mg, 0.14 mmol of azido groups), Pr-OEG$_3$ (43 mg, 0.21 mmol), and PMDETA (30 μL, 0.14 mmol) were dissolved in DMF (3 mL) in a 5-mL vial under nitrogen, followed by adding CuBr (20 mg, 0.14 mmol). The mixture was stirred at room temperature for 24 h. The product was purified by dialyzing against distilled water in a dialysis bag with a cutoff molecular weight of 3000 g mol^{-1}. After drying under vacuum, the product was obtained as a yellow solid. (47 mg, 80% yield). ^{1}H NMR ($CDCl_3$, δ, ppm): 8.29 (s, 1H, N*H*), 7.73 (s, 1H, —NC*H*═C), 4.55 (s, 2H, C═CCH_2O—), 4.36 (s, 2H, —OCH_2CH$_2$CH$_2$N—), 4.01 (s, 2H, —OCH$_2$CH$_2$CH_2N), 3.93 (s, 1H, —COC*H*NH—), 3.56 (m, 8H, —OCH_2CH_2O—), 3.27 (s, 3H, —CH_3), 2.58 (s, 2H, —CH$_2$CH_2COO—), 2.35 (s, 2H, —CH_2CH$_2$COO—) and 2.13(s, 2H, —OCH$_2$CH_2CH$_2$N—).

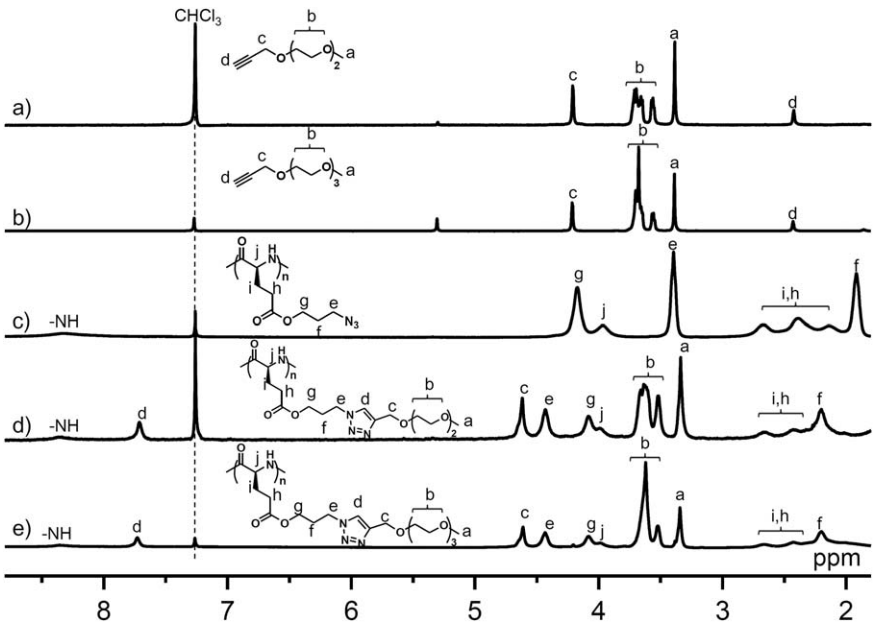

Figure 1. ^{1}H NMR spectra of (a) Pr-OEG$_2$, (b) Pr-OEG$_3$, (c) PAPLG$_{88}$, (d) PPLG$_{88}$-g-OEG$_2$, and (e) PPLG$_{88}$-g-OEG$_3$.

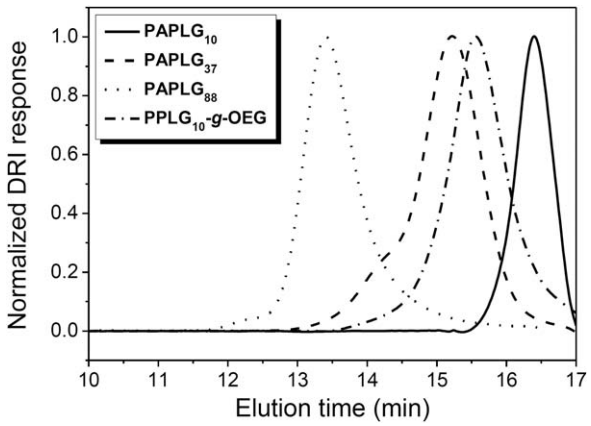

Figure 2. Representative GPC chromatograms of PAPLGs (DP = 10, 37 and 88) and $PPLG_{10}$-g-OEG_3.

RESULTS AND DISCUSSION

Poly(γ-propyl-L-glutamate)-graft-(oligo-ethylene-glycol)s (PPLG-g-OEGs) were synthesized via copper-mediated 1,3-dipolar cycloaddition between poly(γ-3-azidopropyl-L-glutamate)s (PAPLGs) and propargyl functionalized oligo ethylene glycols (Pr-OEGs) (Scheme 1). Pr-OEG side chains [Figure 1(a,b)] were prepared form propargyl bromide and oligo ethylene glycols via etherification reactions.[22] PAPLGs [Figure 1(c)] were synthesized by ring-opening polymerizations of γ-chloropropyl-L-glutamate based N-carboxyanhydride (CP-NCA) and post-modification of poly(γ-chloropropyl-L-glutamate)s (PCPLGs) with NaN_3.[20,21] PAPLGs with different number average molecular weights (M_ns) and molecular weight distributions (PDIs) were obtained by changing initial monomer to initiator ratios (i.e., n-butylamine) in the ring-opening polymerization step. The M_ns of PAPLGs were determined by GPC (Figure 2), which was calibrated with polystyrene standards.

The molecular structures of PPLG-g-OEGs were verified by ^{1}H NMR, GPC, and FTIR. For examples, in the ^{1}H NMR spectra [Figure 1(d,e)], the appearance of chemical resonance at 7.7 ppm suggests the formation of triazole groups after click reactions. In the GPC curves (Figure 2), a noticeable peak shift can be observed by comparing $PAPLG_{10}$ sample with $PPLG_{10}$-g-OEG_2 sample, which suggests an increase of M_n after grafting PEG side-chains. In the FTIR spectra, Pr-OEGs [1, 2 in Figure 3(a)] show characteristic bands at 2875, 2116, and 1097 cm^{-1} corresponding to ν_{C-H}, ν_{alkyne}, and ν_{C-O-O}, respectively. Additionally, PAPLGs [3, 4, and 5 in Figure 3(a)] exhibit ν_{N-H}, $\nu_{N=N=N}$, and $\nu_{C=O}$ of ester bonds at 3290, 2090, and 1735 cm^{-1}, respectively. In the FTIR spectra of PPLG-g-OEGs, the absence of $\nu_{N=N=N}$ and appearance of ν_{C-O-O} suggest the successful grafting of OEG side-chains to the polypeptide backbones with nearly quantitative grafting efficiency.

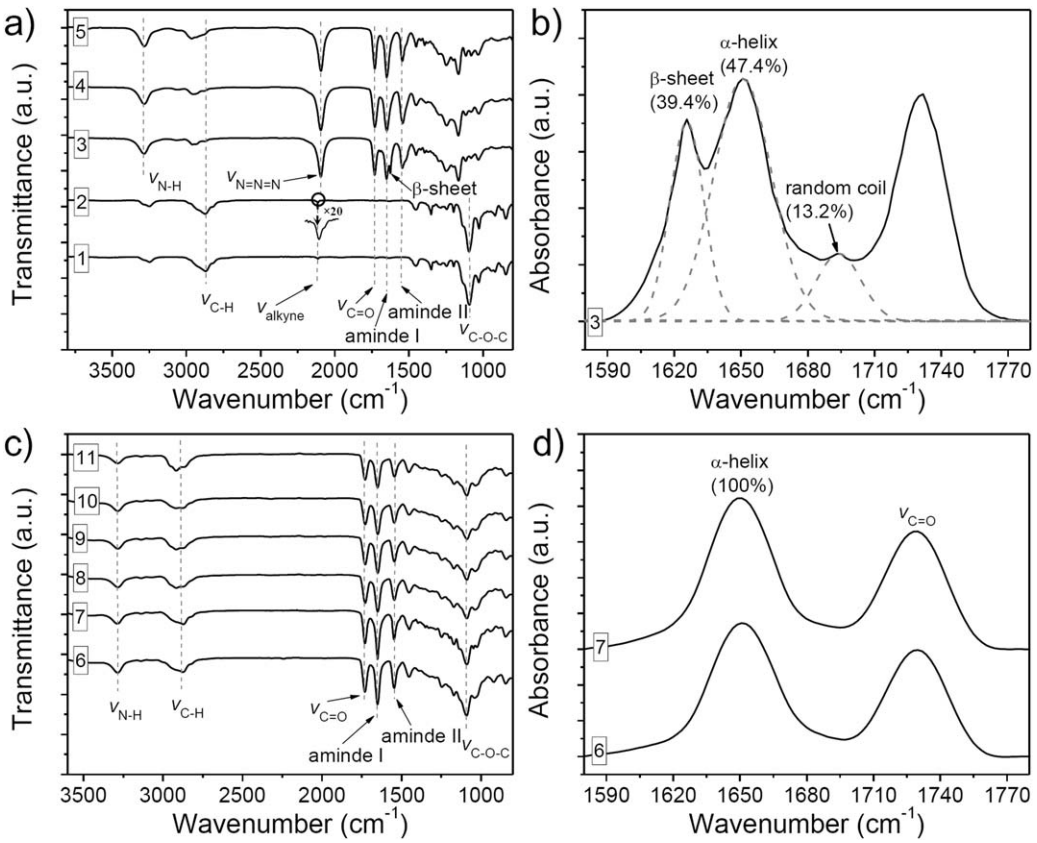

Figure 3. (a and c) Full and (b and d) expanded FTIR spectra of Pr-OEG_m (m = 2 and 3, correspond to curve 1 and 2), $PAPLG_n$ (n = 10, 37 and 88, correspond to curve 3, 4 and 5), $PPLG_n$-g-OEG_2 (n = 10, 37 and 88, correspond to curve 6–8), and $PPLG_n$-g-OEG_3 (n = 10, 37, and 88, correspond to curve 9–11). (b) $PAPLG_{10}$ with Gaussian fitting curves (dotted lines).

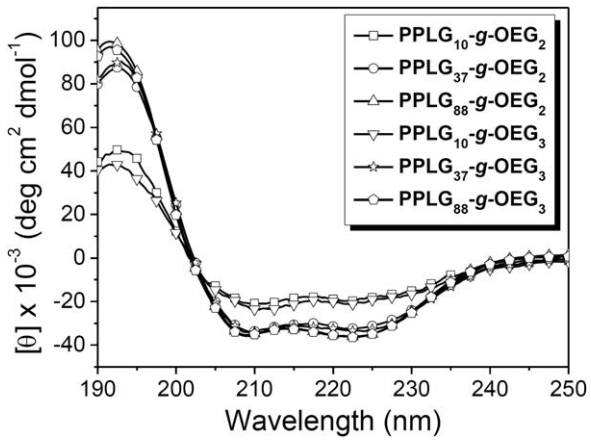

Figure 4. CD spectra of $PPLG_n$-g-OEG_m ($n = 10$, 37, and 88; $m = 2$ and 3).

The secondary structures of PPLG-g-OEGs in solid state were studied by FTIR spectroscopy. Typically, polypeptides adopted α-helical, β-sheet, or random-coil conformations show characteristic amide I bands at around 1655, 1625, and 1690 cm^{-1}, respectively.[25] In the FTIR spectra [Figures 2(a) and 3(c)], $PAPLG_{10}$ with short main-chain length (DP = 10) shows two amide I bands at 1656, 1628, and 1690 cm^{-1} suggesting heterogeneous conformations of α-helix, β-sheet, and random coil. The relative content of α-helix (47.4%), β-sheet (39.4%), and random coil (13.2%) can be quantified by fitting these characteristic peaks using Gaussian distribution [Figure 3(c)]. PAPLGs with long main-chain length (DP = 37 and 88) adopt 100% α-helix in the solid state. The chain-length dependent conformation of PAPLGs is similar to that of PBLGs in the solid state.[26] In comparison, PPLG-g-OEGs with both short and long main-chain lengths exhibited only α-helical conformation [Figure 3(b,d)] in the solid state, suggesting an increased α-helical conformation by incorporation of OEG side-chains.

The solution (i.e., water) conformation of PPLG-g-OEGs with different main-chain and side-chain length was characterized by CD spectroscopy (Figure 4). All the samples adopt α-helical conformations in aqueous solutions, as verified by the characteristic negative ellipticity minima at 208 and 222 nm, and a positive ellipticity maximum at 190 nm.[27] The fractional helicity (f_H) of the resulting polypeptides was calculated using eq. (1)[24] to allow for a quantitative comparison of the relative helical content in PPLG-g-OEGs:

$$f_H = \left(-[\theta]_{222} + 3000\right)/39,000 \quad (1)$$

where $[\theta]_{222}$ is the mean residue ellipticity at 222 nm.

The f_H of PPLG-g-OEGs is in the range of 50∼100% (Table I). It increases as increasing the main-chain length, which is probably resulted from the enhancement of cooperative folding as the main-chain length increase.

The thermoresponsive behaviors of PPLG-g-OEGs in aqueous solutions were studied by DLS. PPLG-g-OEGs are highly soluble in water below cloud point temperature (T_{cp}). The side-chains (i.e., OEGs) start to dehydrate at T_{cp}, which leads to a sharp transition in the light scattering intensity (Figure 5). The T_{cp} can be determined from the intersection of two linear fitting curves to the scattering intensities before and after the transition [Figure 5(a)]. The T_{cp} slightly decreased (by 1.8°C) when polymer (i.e., $PPLG_{37}$-g-OEG_3) concentration increased from 4 to 20 mg mL^{-1} [Figure 5(a–c)], which resulted from the increased intermolecular aggregation. Additionally, we observed that the opaque solution of PPLG-g-OEG became clear again after cooling down to the temperature below T_{cp}, suggesting a reversible thermoresponsive behavior, which has been verified by DLS [Figure 5(d)]. No hysteresis was observed in a heating/cooling cycle [Figure 5(d)], suggesting that PPLG-g-OEG adopted a less compact conformation (e.g., small aggregation size and weak intermolecular interactions) allowing a fast reversible response. By comparison, the thermoresponsive polymer aggregations formed by intra- and/or intermolecular H-bonds exhibited hysteresis in the heating/cooling cycle, which resulted from a more compact conformation (e.g., large aggregation size and strong intermolecular interactions).[28,29]

The effect of main-chain and side-chain length on the T_{cp}s was also revealed by DLS (Figure 6). We found that $PPLG_{10}$-g-OEG_m ($m = 2$ and 3) showed no solution phase transition in

Table I. Molecular Structure Parameters of PPLG-g-OEGs, and Their Helicities and Cloud Point Temperatures in Water

	$PPLG_n$-g-OEG_m					
Entry	M_n [a]	M_w/M_n [b]	n[c]	m[d]	Helicity (%)	T_{cp}[e] (°C)
1	3700	1.10	10	2	50	-
2	13700	1.17	37	2	91	39.5
3	32600	1.04	88	2	100	33.5
4	4100	1.10	10	3	54	-
5	15300	1.17	37	3	93	59.7
6	36500	1.04	88	3	100	56.3

[a] Number average molecular weight (M_n) of PPLG-g-OEGs calculated from the M_n of the main-chain plus the molecular weight of Pr-OEG × the degree of polymerization (DP) of PAPLG.
[b] Molecular weight distribution of PAPLGs determined by GPC (0.01*M* LiBr/DMF) using polystyrene standards.
[c] DP of PAPLGs determined by GPC.
[d] DP of OEGs.
[e] The cloud point temperature of PPLG-g-OEG aqueous solution at 4 mg mL^{-1}, which was determined by DLS.

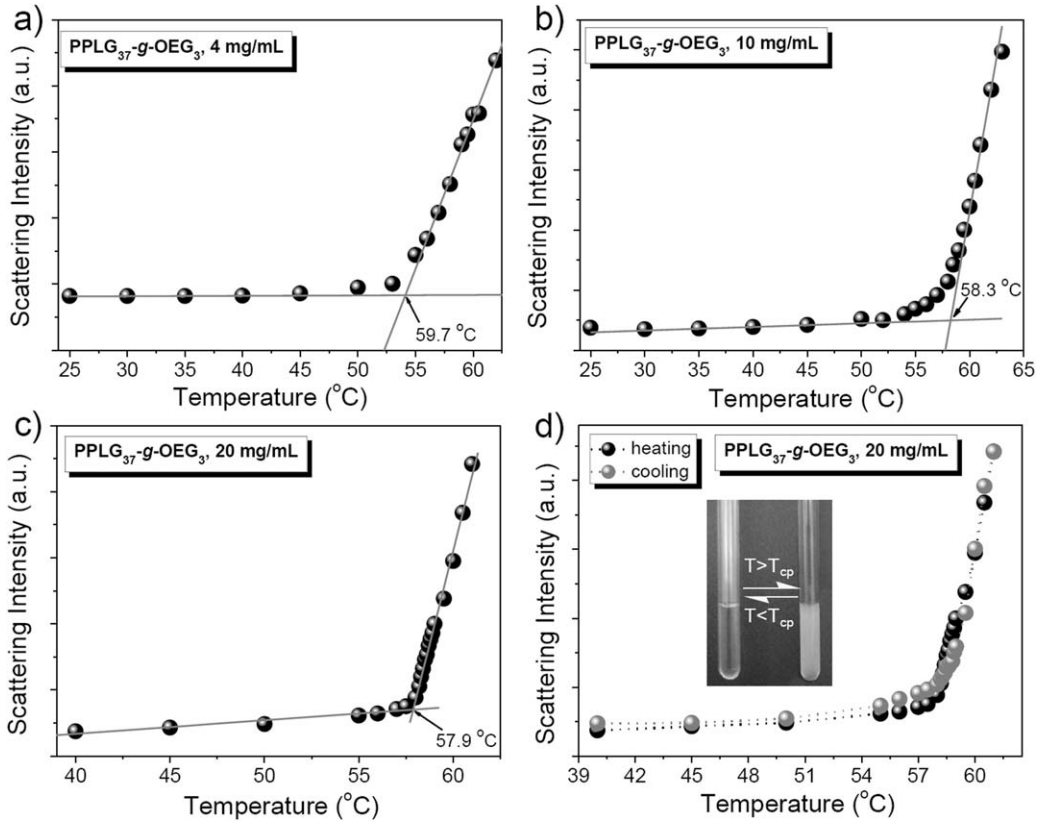

Figure 5. Light scatting intensity of $PPLG_{37}$-g-OEG_3 aqueous solutions at (a) 4 mg mL^{-1}, (b) 10 mg mL^{-1}, and (c) 20 mg mL^{-1} as a function of temperature in the heating cycle. (d) Representative DLS result of $PPLG_{37}$-g-OEG_3 aqueous solution (20 mg mL^{-1}) in a heating/cooling cycle and an optical image to show reversible thermoresponsive behavior of $PPLG_{37}$-g-OEG_3 aqueous solution. The spherical symbols and lines signify the DLS data and linear fitting curves.

the temperature range between 0 and 100°C. While the reason is not clear yet, we tentatively ascribe this to the low helicity (~50%) of $PPLG_{10}$-g-OEG_m.[16,30] PPLG-g-OEGs with longer main-chain lengths (DP ≥ 37) and high helicities (>90%) show T_{cp}s in the range of 33.5~59.7°C in water at 4 mg·mL^{-1}. Increasing the main-chain length can decrease the T_{cp}s. For example, $PPLG_{37}$-g-OEG_2 shows a T_{cp} at 39.5°C (Table I, entry 2) while $PPLG_{88}$-g-OEG_2 shows a T_{cp} at 33.5°C (Table I, entry 3). This is probably because thermoresponsive polymers with longer main-chain length facilitate their aggregations at the transition temperatures.[18] Increasing the side-chain length can significantly increase the T_{cp}s due to the increased side-chain hydrophilicity. For instance, $PPLG_{37}$-g-OEG_2 shows a T_{cp} at 39.5°C (Table I, entry 2) and $PPLG_{37}$-g-OEG_3 shows a T_{cp} at 59.7°C (Table I, entry 5). Additionally, we noticed that T_{cp}s of PPLG-g-OEG aqueous solutions were lower than those of PPLG-g-MEGs.[18] For example, T_{cp} of $PPLG_{37}$-g-OEG_3 aqueous solution (10 mg·mL^{-1}) is 58.3°C while T_{cp} of $PPLG_{37}$-g-MEG_3 is in the range of 74~60°C,[18] suggesting that the T_{cp}s are highly sensitive to their side-chain structures.

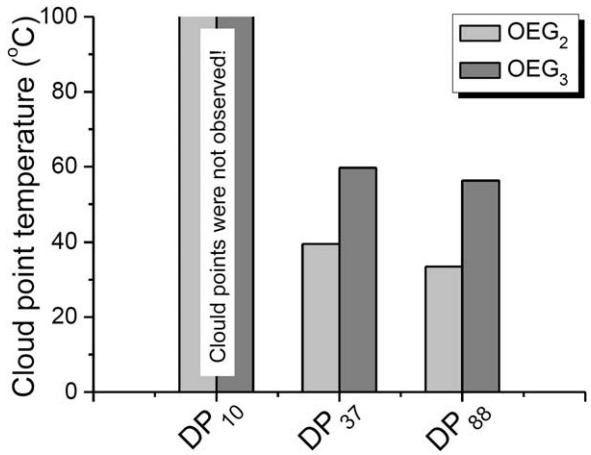

Figure 6. The plot of the cloud point temperature versus the main-chain length of PPLG-g-OEGs at 4 mg mL^{-1} in water.

CONCLUSIONS

In this study, we have demonstrated that the PPLG-g-OEGs with different main-chain and side-chain lengths were readily prepared by click reaction between PAPLG and Pr-OEGs with a nearly quantitative grafting efficiency. PPLG-g-OEGs adopt α-helical conformations both in the solid states and aqueous solutions. OEG side-chains can stabilize the α-helical conformation of PPLG-g-OEGs with short main-chain length (DP = 10). DLS results revealed reversible thermoresponsive properties of PPLG-g-OEGs in aqueous solutions. The cloud point temperature (T_{cp}) increased by increasing the polymer concentration

and OEG side-chain length, or by decreasing the polypeptide main-chain length. These thermoresponsive polypeptides we prepared will have great potential application in the field of biomedical materials.

ACKNOWLEDGMENTS

This work is supported by National Natural Science Foundation of China (Grant 21204075), Hunan Provincial Natural Science Foundation of China (13JJ6042), and Xiangtan University start-up fund (12QDZ06).

REFERENCES

1. Weber, C.; Hoogenboom, R.; Schubert, U. S. *Prog. Polym. Sci.* **2012**, *37*, 686.
2. Motornov, M.; Roiter, Y.; Tokarev, I.; Minko, S. *Prog. Polym. Sci.* **2010**, *35*, 174.
3. Luo, Y.-L.; Yang, X.-L.; Xu, F.; Chen, Y.-S.; Ren-Ting, Z.-M. *J. Appl. Polym. Sci.* **2013**, *130*, 4137.
4. Wang, Y.; Wang, J.; Ge, L.; Liu, Q.; Jiang, L.; Zhu, J.; Zhou, J.; Xiong, F. *J. Appl. Polym. Sci.* **2013**, *127*, 3749.
5. Chen, S.; Jiang, X.; Sun, L. *J. Appl. Polym. Sci.* **2013**, *130*, 1164.
6. Wei, Q.-B.; Luo, Y.-L.; Fu, F.; Zhang, Y.-Q.; Ma, R.-X. *J. Appl. Polym. Sci.* **2013**, *129*, 806.
7. Wever, D. A. Z.; Riemsma, E.; Picchioni, F.; Broekhuis, A. A. *Polymer* **2013**, *54*, 5456.
8. Wever, D. A. Z.; Ramalho, G.; Picchioni, F.; Broekhuis, A. A. *J. Appl. Polym. Sci.* **2014**, *131*, 39785.
9. Smith, A. E.; Xu, X.; McCormick, C. L. *Prog. Polym. Sci.* **2010**, *35*, 45.
10. Deming, T. *J. Prog. Polym. Sci.* **2007**, *32*, 858.
11. Deng, C.; Wu, J.; Cheng, R.; Meng, F.; Klok, H.-A.; Zhong, Z. *Prog. Polym. Sci.* **2014**, *39*, 330.
12. Deming, T. *J. Adv. Polym. Sci.* **2006**, *202*, 1.
13. Hadjichristidis, N.; Iatrou, H.; Pitsikalis, M.; Sakellariou, G. *Chem. Rev.* **2009**, *109*, 5528.
14. He, C.; Zhuang, X.; Tang, Z.; Tian, H.; Chen, X. *Adv. Healthcare Mater.* **2012**, *1*, 48.
15. Huang, J.; Heise, A. *Chem. Soc. Rev.* **2013**, *42*, 7373.
16. Chen, C.; Wang, Z.; Li, Z. *Biomacromolecules* **2011**, *12*, 2859.
17. Fu, X.; Shen, Y.; Fu, W.; Li, Z. *Macromolecules* **2013**, *46*, 3753.
18. Cheng, Y.; He, C.; Xiao, C.; Ding, J.; Zhuang, X.; Chen, X. *Polym. Chem.* **2011**, *2*, 2627.
19. Ding, J.; Zhao, L.; Li, D.; Xiao, C.; Zhuang, X.; Chen, X. *Polym. Chem.* **2013**, *4*, 3345.
20. Tang, H.; Zhang, D. *Biomacromolecules* **2010**, *11*, 1585.
21. Hu, Q.; Deng, Y.; Yuan, Q.; Ling, Y.; Tang, H. *J. Polym. Sci. Part A: Polym. Chem.* **2014**, *52*, 149.
22. Deng, Y.; Hu, Q.; Yuan, Q.; Wu, Y.; Ling, Y.; Tang, H. *Macromol. Rapid Commun.* **2014**, *35*, 97.
23. Kelly, S. M.; Jess, T. J.; Price, N. C. *Biochim. Biophys. Acta* **2005**, *1751*, 119.
24. Morrow, J. A.; Segall, M. L.; Lund-Katz, S.; Phillips, M. C.; Knapp, M.; Rupp, B.; Weisgraber, K. H. *Biochemistry* **2000**, *39*, 11657.
25. Susi, H.; Timasheff, S. N.; Stevens, L. *J. Biol. Chem.* **1967**, *242*, 5460.
26. Papadopoulos, P.; Floudas, G.; Klok, H. A.; Schnell, I.; Pakula, T. *Biomacromolecules* **2004**, *5*, 81.
27. Screerama, N.; Woody, R. W., Eds. Circular Dichroism Principle and Application; VCH-Wiley: New York, **2000**.
28. Kujawa, P.; Aseyev, V.; Tenhu, H.; Winnik, F. M. *Macromolecules* **2006**, *39*, 7686.
29. Qiao, Z.-Y.; Du, F.-S.; Zhang, R.; Liang, D.-H.; Li, Z.-C. *Macromolecules* **2010**, *43*, 6485.
30. Hwang, J.; Deming, T. *J. Biomacromolecules* **2001**, *2*, 17.